Hormones and Behavior 106 (2018) 178–188

Contents lists available at ScienceDirect

Hormones and Behavior

journal homepage: www.elsevier.com/locate/yhbeh

Neural activity in the social decision-making network of the brown anole during reproductive and agonistic encounters

David Kabelik[a,b,*], Chelsea A. Weitekamp[c], Shelley C. Choudhury[a,b], Jacob T. Hartline[a,b], Alexandra N. Smith[a,b], Hans A. Hofmann[c,d,e]

[a] Department of Biology, Rhodes College, Memphis, TN 38112, USA
[b] Program in Neuroscience, Rhodes College, Memphis, TN 38112, USA
[c] Department of Integrative Biology, University of Texas at Austin, Austin, TX 78712, USA
[d] Institute for Cellular and Molecular Biology, University of Texas at Austin, Austin, TX 78712, USA
[e] Institute for Neuroscience, University of Texas at Austin, Austin, TX 78712, USA

ARTICLE INFO

Keywords:
Anolis
Lizard
Courtship
Aggression
Vasotocin
Vasopressin
Mesotocin
Oxytocin
Catecholamines
Serotonin

ABSTRACT

Animals have evolved flexible strategies that allow them to evaluate and respond to their social environment by integrating the salience of external stimuli with internal physiological cues into adaptive behavioral responses. A highly conserved social decision-making network (SDMN), consisting of interconnected social behavior and mesolimbic reward networks, has been proposed to underlie such adaptive behaviors across all vertebrates, although our understanding of this system in reptiles is very limited. Here we measure neural activation across the SDMN and associated regions in the male brown anole (*Anolis sagrei*), within both reproductive and agonistic contexts, by quantifying the expression density of the immediate early gene product Fos. We then relate this neural activity measure to social context, behavioral expression, and activation (as measured by colocalization with Fos) of different phenotypes of 'source' node neurons that produce neurotransmitters and neuropeptides known to modulate SDMN 'target' node activity. Our results demonstrate that measures of neural activation across the SDMN network are generally independent of specific behavioral output, although Fos induction in a few select nodes of the social behavior network component of the SDMN does vary with social environment and behavioral output. Under control conditions, the mesolimbic reward nodes of the SDMN actually correlate little with the social behavior nodes, but the interconnectivity of these SDMN components increases dramatically within a reproductive context. When relating behavioral output to specific source node activation profiles, we found that catecholaminergic activation is associated with the frequency and intensity of reproductive behavior output, as well as with aggression intensity. Finally, in terms of the effects of source node activation on SDMN activity, we found that Ile^{8}-oxytocin (mesotocin) populations correlate positively, while Ile^{3}-vasopressin (vasotocin), catecholamine, and serotonin populations correlate negatively with SDMN activity. Taken together, our findings present evidence for a highly dynamic SDMN in reptiles that is responsive to salient cues in a social context-dependent manner.

1. Introduction

All animals encounter challenges (e.g., territorial intrusions; competition for mates) as well as opportunities (e.g., finding a mate; ascending to social dominance) throughout their lives. Their behavioral decisions in these situations fundamentally affect their chances of survival and reproduction (O'Connell and Hofmann, 2011a; Rittschof and Robinson, 2016). O'Connell and Hofmann (2011b) proposed that a relatively conserved social decision-making network (SDMN; see Table 1 for list of abbreviations), consisting of overlapping social behavior and mesolimbic reward system neural networks, underlies these decision-making processes, allowing vertebrates to evaluate the salience and valence of stimuli in relation to their life history. Changes in neural activity at nodes within this network are associated with corresponding changes in behavioral expression. This nodal activity is modulated by a number of signaling molecules (e.g., nonapeptides, catecholamines, indolamines, steroid hormones) that have been shown to regulate social behaviors on an individual basis, and differently within different social contexts (Crews, 2003; Goodson, 2005; Goodson and Kabelik, 2009; Newman, 1999; O'Connell and Hofmann, 2012; Yang and Wilczynski,

* Corresponding author at: Department of Biology, Rhodes College, 2000 N Parkway, Memphis, TN 38112, USA.
E-mail addresses: kabelikd@rhodes.edu (D. Kabelik), hans@utexas.edu (H.A. Hofmann).

https://doi.org/10.1016/j.yhbeh.2018.06.013
Received 28 July 2017; Received in revised form 21 June 2018; Accepted 28 June 2018
Available online 26 October 2018
0018-506X/

Table 1
List of abbreviations.

5-HT	5-hydroxytryptamine (serotonin)
A11 midd	dorsal midline A11 catecholaminergic neurons
A11 midv	ventral midline A11 catecholaminergic neurons
A1C1	catecholaminergic area A1/C1
LC/SC	locus coeruleus/sub-coeruleus area
A8	A8 catecholaminergic area
AH	anterior hypothalamus
AMYbl	basolateral amygdala
AMYc	cortical amygdala
AMYm	medial amygdala
AOI	area of interest
BNST	bed nucleus of the stria terminalis
CN	cochlear nucleus
DA	dopamine
Epi	epinephrine
flm	medial longitudinal fasciculus
ir	immunoreactive
LH	lateral hypothalamus
LS	lateral septum
NAc	nucleus accumbens
NE	norepinephrine
NST	nucleus of the solitary tract
OT	oxytocin
PAG	periaqueductal (a.k.a., central) gray
PH-AH	periventricular hypothalamus-anterior hypothalamus region
POA	preoptic area
PVN	paraventricular nucleus of the hypothalamus
RAi	inferior raphe
RAic	inferior raphe, caudal division
RAs	superior raphe
RAsl	superior raphe, lateral division
RAsm	superior raphe, medial division
RSL	reticular nucleus, lateral
RSM	reticular nucleus, medial
SDMN	social decision-making network
SN	substantia nigra
SON	supraoptic nucleus of the hypothalamus
TH	tyrosine hydroxylase
TS	torus semicircularis
VAA	ventral anterior amygdala
VMH	ventromedial nucleus of the hypothalamus
VMS	ventromedial septum
VP	vasopressin
VTA	ventral tegmental area

2002). Furthermore, the functional connectivity of nodes within the network can be influenced by social environment, at least partly via signaling molecules – e.g., via the nonapeptide oxytocin during reproductive opportunities (Johnson et al., 2016). However, much remains unknown about how various other social environments, and different signaling molecules originating from and targeting different brain regions, affect neural activity across the multitude of nodes of the SDMN. Even whether a functional SDMN is present across all vertebrate groups has been questioned (Goodson and Kingsbury, 2013). We here present evidence for a functional SDMN in reptiles, and examine neural activity differences, as well as differences in functional connectivity to and within this network, across and within Reproductive (including courtship and intromission), Agonistic (relating to conflict), and Control (solitary, non-social) environments in the male brown anole lizard (*Anolis sagrei*).

While birds and mammals are well-researched in the field of behavioral neuroscience, reptiles remain relatively overlooked; in fact the study of behavioral neuroscience in reptiles also lags that of amphibians, fish, and invertebrates (Kabelik and Hofmann, this issue; Taborsky et al., 2015). This lack of research on reptiles is a significant problem for understanding the evolution and function of the vertebrate SDMN, given reptiles' important position in vertebrate phylogeny. Examination of lizards is important for evolutionary comparisons among amniotic vertebrates (mammals, birds, and reptiles). Mammals evolved from reptile-like synapsids, while all other extant amniotes evolved from diapsids, with lizards and other squamates constituting the majority of the Lepidosauria, a separate group from the Archelosauria (Archosauromorpha) which comprise birds, crocodiles, and likely also turtles (Crawford et al., 2015).

By examining a small vertebrate brain (that of the brown anole lizard), and implementing immunofluorescent detection of chemoarchitecture and a marker of neural activity (the production of the immediate early gene product Fos), we here present an analysis of neural activity at various source signaling molecule cell clusters ('source' nodes), as well as at 'target' SDMN nodes that are regulated by the neurotransmitters and neuropeptides originating from the source nodes.

The target nodes examined in the present study primarily include brain nuclei that have been specified as part of the SDMN (O'Connell and Hofmann, 2011b) (Fig. 1). The nodes include components of the social behavior network such as the preoptic area (POA), anterior hypothalamus (AH), ventromedial nucleus of the hypothalamus (VMH) and periaqueductal gray (PAG; a.k.a., central gray), as well parts of the mesolimbic reward system such as the nucleus accumbens (NAc), the basolateral amygdala (AMYbl, often described in reptiles as the posterior dorsal ventricular ridge but a presumed homologue of the mammalian AMYbl, (Lanuza et al., 1998; Martínez-García et al., 2002)), and the ventral tegmental area (VTA). Examined brain regions that are part of both networks include the lateral septum (LS) and the bed nucleus of the stria terminalis (BNST)/medial amygdala (AMYm) continuum. Additional regions examined within this study include the ventromedial septum (VMS), which is a distinct septal region in lizard brains that possesses strong connectivity with the AH as well as with the BNST and parts of the amygdala (Font et al., 1997, 1998). We also examine the cortical amygdala (AMYc, a.k.a., ventral anterior amygdala, which is thought to be homologous to the mammalian anterior and posterolateral cortical amygdala, Martínez-García et al., 2002), and the paraventricular nucleus of the hypothalamus (PVN; implicated in stress responsiveness, Goodson and Kabelik, 2009; Goodson and Kingsbury, 2013). Furthermore, we examined the substantia nigra (SN) and the location of the A8 catecholamine population, both additional dopaminergic midbrain sites that are part of the mesolimbic reward system along with the VTA. We also examined activity in the torus semicircularis (TS), as it is continuous with the PAG and possesses some behavioral functions. Although parts of the TS are at least partly homologous to the inferior colliculus (Butler and Hodos, 2005), and thus likely possesses some auditory function, the TS also possesses other roles that make it important for inclusion in the SDMN. For instance, the TS is an intermediary relay area between the LS and the PAG (Font et al., 1998). Sex steroid hormone receptors are also present in the TS of anoles (Morrell et al., 1979), and electrical stimulation of the TS in the green iguana (*Iguana iguana*) has been shown to elicit dewlap displays (Distel, 1978). The TS regions sampled here have also been shown to express substance P, as does the lateral PAG of mammals (Goodson and Kingsbury, 2013), raising the possibility that these regions are also partly homologous.

In the present study, the signaling molecules that were visualized directly include the lizard vasopressin (VP; Ile^3-vasopressin, a.k.a. Arg^8-vasotocin) and the lizard oxytocin (OT; Ile^8-oxytocin, a.k.a. mesotocin). We use the terms vasopressin and oxytocin here, rather than vasotocin and mesotocin, according to the example of Kelly and Goodson (2014), to denote homology with the mammalian forms of the nonapeptides from which they vary solely by one amino acid substitution; in mammals, equivalent differences do not constitute deviations from this nomenclature (e.g., Arg^8-vasopressin and Lys^8-vasopressin are both referred to as vasopressin, while Leu^8-oxytocin and Pro^8-oxytocin are both referred to as oxytocin) (Albers, 2015; Lee et al., 2011). We also directly examined neurons producing the indolamine serotonin (5-hydroxytryptamine, 5-HT). Furthermore, we examined neurons producing the catecholamines dopamine (DA), norepinephrine (NE), and epinephrine (Epi) by means of visualizing the rate-limiting enzyme in

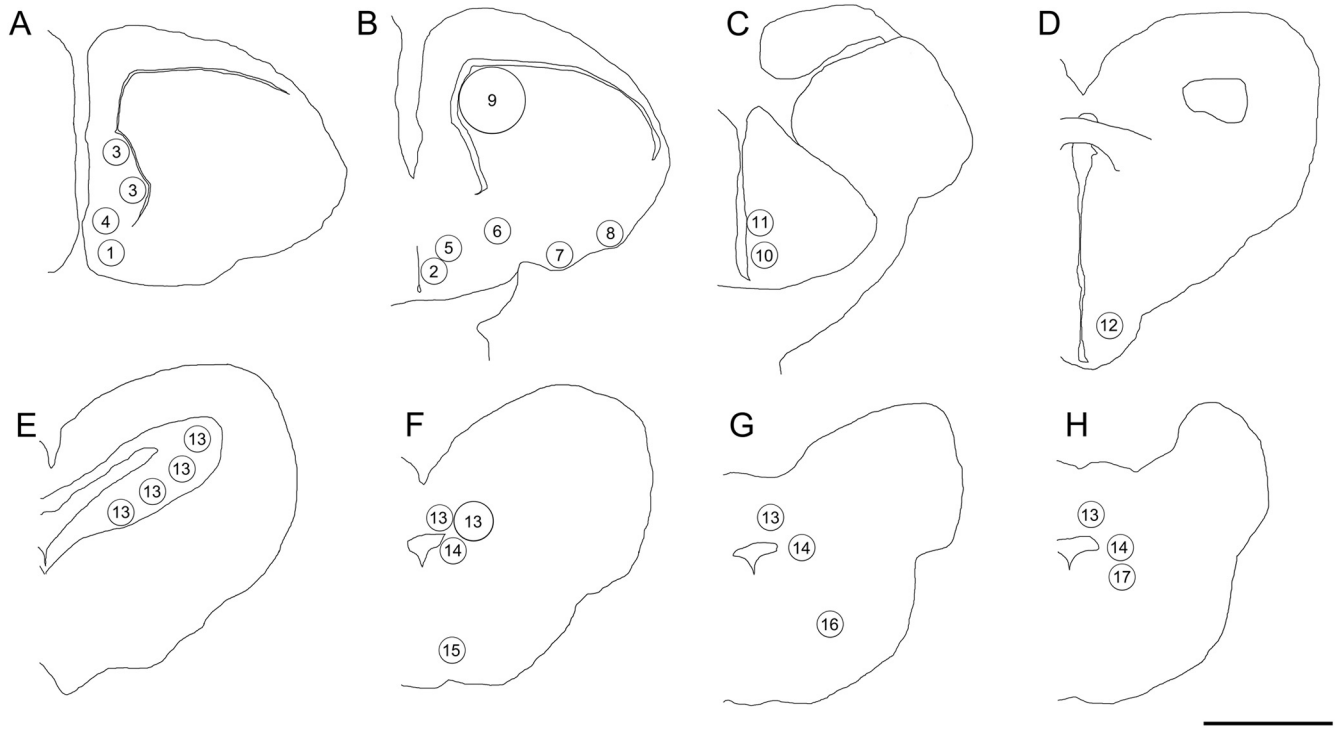

Fig. 1. A map of the examined SDMN ('target') nodes. A series of traced images of select forebrain (A–D) and midbrain (E–H) sections from an experimental brain in this study depicts the target regions that were sampled for Fos-ir density. Relative to the rostral-caudal position of the first opening of the third ventricle within the preoptic area, which we use as our zero coordinate, these sections come at: A, −0.4 mm; B, +0.1 mm; C, +0.6 mm; D, +1.3 mm; E, +1.8 mm; F, +2.1 mm; G, +2.3 mm; H, +2.4 mm. The areas of interest (AOIs) within which sampling occurred are: 1, NAcc; 2, POA; 3-4, LS; 4, VMS; 5, BNST; 6, BNST-AMYm transition zone; 7, AMYm; 8, AMYc; 9, AMYbl; 10, AH; 11, PVN; 12, VMH; 13, TS; 14, PAG; 15, VTA; 16, SN; 17, A8. Scale bar represents 1 mm.

catecholamine synthesis, tyrosine hydroxylase (TH). Neural activity within these signaling molecule-producing neurons, in relation to social behavior context and behavioral expression in brown anoles, was previously examined separately by means of immunofluorescent colocalization with Fos (Hartline et al., 2017; Kabelik et al., 2013, 2014; Kabelik and Magruder, 2014). Fos is a robust marker of neural activity, and its upregulation is induced both by large-scale neural depolarization and by non-action potential-coupled pathways such as calcium influx due to receptor activation (Sabatier et al., 2003). In the present study, we examine brain sections from these same male brown anoles, but now focus primarily on target SDMN node activation, correlations among the nodes, and how nodal activity and coordination is influenced by source node activity and social context. Specifically, we expose *A. sagrei* males to either a conspecific female (Reproductive opportunity) or a conspecific male (Agonistic challenge) and contrast these treatments to a solitary Control context. Importantly, the Control context still exposes focal males to a novel environment, as in the experimental conditions, but there is no social stimulus present in this novel environment. We predicted that target node activity within the SDMN will generally increase in social versus asocial contexts, but the opposite was found. We also expected and did find correlated activation of select SDMN nodes with increased social behavior expression. Furthermore, we predicted increased functional connectivity (correlated activity) among SDMN nodes in social behavior contexts relative to the Control condition, and found this true for the Reproductive context. Finally, we expected source node activity to correlate in both positive and negative directions with target node activity (depending on the specific brain nucleus and signaling molecule examined), and we did find such results, with oxytocin connections to the SDMN showing a positive correlation while other regulatory molecules correlated negatively to general SDMN activity.

2. Materials and methods

2.1. Subjects and treatment groups

Fifty-seven adult male brown anoles (*Anolis sagrei*) served as experimental subjects and were divided into treatment groups of Control (no conspecific present, N = 12), Reproductive opportunity (female conspecific present, N = 22), and Agonistic challenge (male conspecific present, N = 23). Data obtained from these same animals regarding Fos colocalization with various signaling molecules have previously been reported (Hartline et al., 2017; Kabelik et al., 2013, 2014; Kabelik and Magruder, 2014). Details about housing, behavioral trials, and tissue processing have thus also been reported previously, but we report them briefly here. All animals were obtained from a commercial supplier, housed in glass terraria, and maintained under long-day (14L:10D) conditions. Each terrarium was illuminated by a 40-W full-spectrum fluorescent light suspended 20 cm above a wire-mesh terrarium lid, and supplemental heat was supplied by means of a 60-W incandescent white light bulb suspended 5 cm above the lid. Subjects were confirmed to be in a breeding state by examination of testes after euthanasia for brain harvesting. All procedures involving live animals were conducted according to federal regulations and approved by the Institutional Animal Care and Use Committee at Rhodes College.

2.2. Behavioral trials

Prior to the onset of behavioral trials, the experimental subjects were housed for at least 72 h in one half of a terrarium (30.5 cm H × 26 cm W × 51 cm L), divided into two equal halves (measured along the long edge) by an opaque partition. A focal male was always housed in one terrarium half; the other half was either empty (Control treatment), contained a female (male-female Reproductive opportunity group), or contained a conspecific male that was smaller by one to

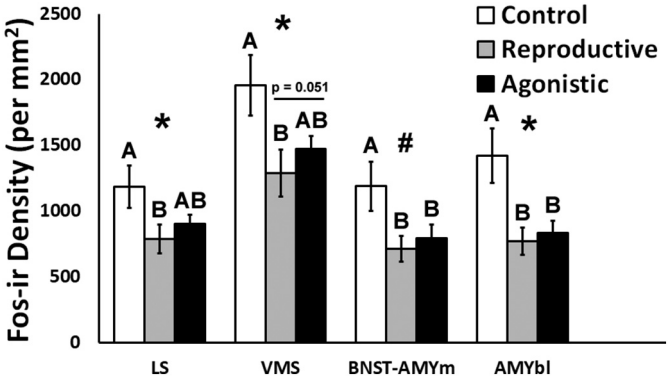

Fig. 2. Neural activity differences at several SDMN nodes across behavioral treatments. Mean Fos-ir density at a number of SDMN nodes differs across social interaction treatments. In pairwise comparisons, subjects in Reproductive opportunities possessed a lower density of Fos-ir at all depicted nodes, while subjects in Agonistic encounters also experienced lower Fos-ir densities in the BNST-AMYm transition zone and the AMYbl. * represents nodes with overall treatment effects at $p < 0.05$; # represents $p = 0.053$. Different letters above bars denote groups differing at $p < 0.05$ in post hoc pairwise comparisons. The Reproductive and Agonistic group measures within the VMS were marginally different at $p = 0.051$.

2 mm snout-vent length (male-male Agonistic challenge group). All animals were kept in visual isolation from others. At the time of a trial, the opaque divider was removed and a 14-min behavioral trial was run. Behaviors were recorded from behind a blind. Behavioral frequency was defined as the sum of engagement behaviors during a 14-min trial, and included head-bob and push-up displays (with and without extension of the dewlap), chases and the consummatory behaviors of either copulation (Reproductive opportunity trials) or biting (Agonistic challenge trials). See Kabelik et al. (2013) for an ethogram describing the recorded behaviors. At the end of the trial, the animals were separated and maintained undisturbed until they were euthanized 90-min from the start time of the behavior trial. This time period is both optimal for peak Fos induction, and sufficient to allow for Fos degradation in instances of reduced Fos induction (Herdegen and Leah, 1998; Hoffman et al., 1993).

2.3. Tissue processing & immunohistochemistry

Brains were removed and fixed by overnight submersion in 4% paraformaldehyde in 0.1 M phosphate buffer at 4 °C, followed by cryoprotection with 30% sucrose in 0.1 M phosphate-buffered saline (PBS). Following freezing, the brains were sectioned into two 50-µm series. Immunohistochemistry was conducted as described in previous publications (Hartline et al., 2017; Kabelik et al., 2013, 2014; Kabelik and Magruder, 2014).

Briefly, series 1 brain sections were processed with 0.1 µg/ml rabbit anti-Fos antibody (Santa Cruz Biotechnology), 0.2 µg/ml of guinea pig anti-vasopressin antibody (Bachem), and 0.5 µg/ml sheep anti-tyrosine hydroxylase antibody (Novus Biologicals). The sections were subsequently processed with donkey anti-rabbit secondary antibody conjugated to Alexa Fluor 488 at 6 µg/ml and donkey-anti-sheep secondary antibody conjugated to Alexa Fluor 680 at 16 µg/ml (both from Life Technologies), as well as donkey-anti guinea-pig secondary antibody conjugated to DyLight 549 at 10 µg/ml (Jackson ImmunoResearch). The series 2 brain sections were processed separately for rostral and caudal portions of each brain. The rostral sections were processed with 1:2000 dilution of a custom rabbit polyclonal anti-oxytocin antibody (VA 10, generously provided by Dr. Harold Gainer, NIH, Bethesda, USA, (Altstein et al., 1988)), 20 µg/ml of mouse monoclonal anti-Fos antibody (Santa Cruz Biotechnology), and 0.1 µg/ml of guinea-pig polyclonal anti-CRF antibody (Bachem; the CRF was part of a separate study). The applied secondary antibodies were a 6 µg/ml dilution of donkey anti-rabbit secondary antibody conjugated to Alexa Fluor 488 (Life Technologies), a 10 µg/ml dilution of donkey anti-mouse secondary antibody conjugated to Alexa Fluor 555 (Life Technologies), and a 16 µg/ml dilution of donkey anti-guinea pig Alexa Fluor 647 (Jackson ImmunoResearch). The caudal sections were processed with the same anti-Fos and anti-CRF antibodies as the rostral sections, but now together with a 1:2000 dilution of goat anti-serotonin polyclonal antibody (Immunostar) as the third primary antibody. The secondary antibodies consisted of the same anti-mouse and anti-guinea pig antibodies as the rostral sections, but now with a 6 µg/ml dilution of donkey anti-goat Alexa Fluor 488 antibody (Life Technologies).

2.4. Microscopy and image analyses

An LSM 700 Confocal microscope and Zen 2010 software (Carl Zeiss), using a 20× objective, were used to capture z-stacks of photomicrographs at 5 µm intervals, in a grid that was later stitched together. A maximum intensity projection created a two-dimensional image. Individual colors were exported as separate layers using AxioVision 4.8 (Carl Zeiss), and these were stacked as overlaid monochromatic layers in Photoshop (Adobe Systems). Layers in the stack could thus be toggled on and off to determine signal colocalization. Analyses were conducted by individuals blind to treatment groups.

2.4.1. Source nodes

A number of VP-immunoreactive (-ir), OT-ir, 5-HT-ir, and TH-ir cells were quantified. Activated neurons were assessed as those exhibiting colocalization with Fos-ir nuclei. Total numbers of cells were not analyzed here because some sections within each series were missing due to damage, and because some nuclei were only analyzed across a set number of sections, while others were analyzed across their full extent. Analyses of colocalization percentages in relation to treatment group and behavioral intensity and frequency have already been reported (Hartline et al., 2017; Kabelik et al., 2013, 2014; Kabelik and Magruder, 2014); these source node colocalization measures are only included in this study to determine correlations with target node activity.

2.4.2. Target nodes

The target node analysis is new to this study and so we describe it here in detail. Fos density throughout the SDMN was assessed by overlaying area of interest (AOI) circles over one or more portions of that brain region (see Fig. 2). These AOIs were of either 0.2, 0.3, or 0.5 mm in diameter, depending on the size and shape of the target node in question. AOIs that contained only a few Fos-ir nuclei on average were counted manually. For AOIs containing many Fos-ir nuclei, a semi-automated analysis using the FIJI program (Schindelin et al., 2012) with a custom script was used to quantify Fos nuclei at these target sites; we describe this process as semi-automated because the selection threshold was set by a user blind to treatment group, while the program then automatically separated overlapping nuclei using a watershed split and counted nuclei that were within the correct size, circularity, and threshold parameters (see Supplementary Fig. 1). This approach was validated by comparisons of manual counting and semi-automated counting across four different AOIs and the mean Pearson's correlation coefficient between the manual and semi-automated approaches was $r = 0.90$. Prior to statistical analysis, the total number of Fos-ir nuclei per AOI was divided by AOI area to generate a standardized measure of Fos-ir density across different AOI sizes, and values from multiple AOI measurements were averaged for each target node. The target node quantification was conducted bilaterally in the NAcc and AMYm across 5 sequential sections, and in the POA and VMH across 4 sections. The BNST, a zone at the intersection of the BNST and AMY that we labelled BNST-AMYm, the AMYc, the AMYbl, the AH, and the VTA were each quantified bilaterally across 3 sections. The PVN

was quantified bilaterally across 2 sections, while the SN and A8 region were each quantified bilaterally across the single section where they were most prominent. Quantification was conducted unilaterally in the dorsal, ventral, and caudal LS across 10 sections (averaged together into a single LS measurement), and the VMS across 8 sections. Four unilateral AOIs per section of the TS were examined across its rostral portion (along the length of the fourth ventricle - up to 4 sections), and then dorsal and dorsolateral to the cerebral aqueduct (also up to 4 sections). Finally, unilateral measurements were made on up to four sections of the PAG.

2.5. Statistical analyses

The data for this study can be found at DOI https://doi.org/10.6084/m9.figshare.6288974. Because some variables did not meet assumptions of parametric analyses, nonparametric analyses were employed throughout this study. Comparisons of treatments and behavioral intensity categories were conducted using Kruskal-Wallis tests, with Mann-Whitney *U* tests used for post hoc pairwise comparisons. Spearman's rho correlations were used for comparisons of continuous variables.

We conducted Principal Component Analyses (PCA) on all the data combined (results not shown). The first two principal components explained only ~37% of the total variation, which indicates that at least the linear proportion of the variation in the data is distributed across many dimensions. The result was similar when we conducted a PCA that only included the Fos-ir densities. As a consequence, dimension reduction does not separate the different treatment groups into obvious clusters, which limits the utility of PCA for the present data set. Instead, to discover and visualize the relationships between behavioral and physiological measures and to generate hypotheses for future study, we created clustered correlation matrices using the R package lattice. Physiological measures included cell counts of overall Fos induction, as well as the fraction of TH, nonapeptide, and 5-HT neurons that express of Fos. Behavior data included frequency, latency, and intensity of aggression and courtship displays. To obtain a complete data matrix, we imputed missing values using the mean with the R package Hmisc (Harrell, 2018). We then used the R package pvclust to generate p-values for each cluster using multiscale bootstrap resampling (Suzuki and Shimodaira, 2006). Clusters for which $p \leq 0.05$ are indicated by a black square.

3. Results

3.1. Analysis of aggression and courtship behavior within treatments

We first examined the latency, frequency, and intensity of aggressive (Agonistic challenge) and courtship (Reproductive opportunity) displays (Supplementary Fig. 2). Because all three behavioral measures were strongly correlated (see Spearman correlation coefficients and p-values in Supplementary Table 1), we used behavioral frequencies as the sole measure in analyses correlating behaviors to Fos-ir density measurements within various brain nuclei.

3.2. Between-treatment and within-treatment analyses of SDMN activity (Fos-ir density)

Next, we examined Fos-ir densities in SDMN nodes of male brown anoles across treatment groups. We found that Fos-ir densities were significantly lower in several SDMN target nodes of individuals exposed to a social encounter (Agonistic or Reproductive) than in the Control treatment (Fig. 2). Specifically, this was the case with the LS ($\chi^2 = 7.14$, df = 2, $p = 0.028$), VMS ($\chi^2 = 8.33$, df = 2, $p = 0.016$), AMYbl ($\chi^2 = 8.09$, df = 2, $p = 0.018$), and marginally also for the BNST-AMYm ($\chi^2 = 5.86$, df = 2, $p = 0.053$). Post hoc pairwise comparisons revealed that in all of these analyses, the Reproductive opportunity group exhibited lower Fos-ir densities than the Control group; in the BNST-AMYm and AMYbl, the Agonistic group also showed lower Fos-ir densities than the Control group. Importantly, Fos-ir densities did not differ between Reproductive and Agonistic encounter treatments in most of these post hoc tests, except for a marginally significant reduction of Fos-ir density in the VMS of Reproductive opportunity individuals compared to Agonistic challenge individuals ($p = 0.051$). No treatment effects or trends were found for the other target nodes ($p > 0.09$ for all). Fos-ir densities at all SDMN nodes are

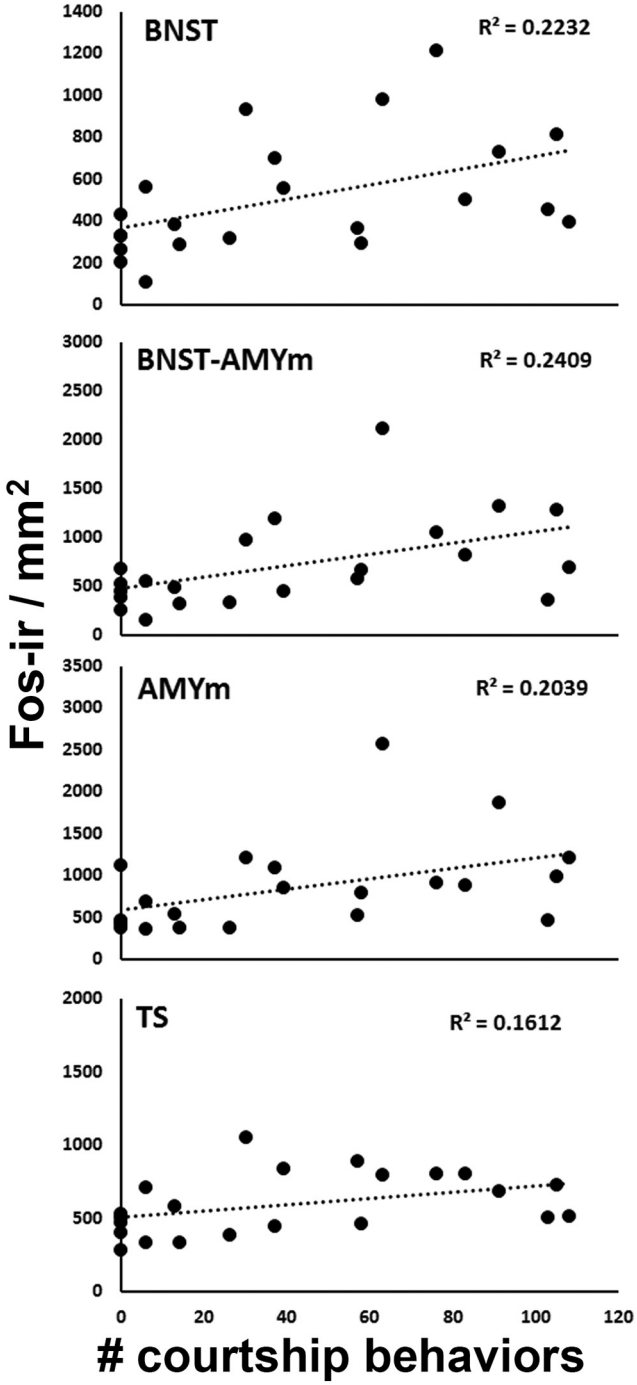

Fig. 3. Neural activity at several SDMN nodes correlates with courtship behavior frequency. Correlations between courtship behavior frequency (total occurrences of head bob, push up, dewlap extension, dewlap extension with push up, chase, and copulate within a 14-min behavioral encounter with a female conspecific) and Fos-ir density per mm^2 were significant at the BNST, BNST-AMYm transition zone, AMYm, and TS. See text for statistical results.

shown in Supplementary Fig. 3.

Fos-ir density was correlated with courtship behavior in several SDMN nodes (Fig. 3). This was true for the BNST ($r_s = 0.57$, N = 22, $p = 0.006$), BNST-AMYm ($r_s = 0.56$, N = 22, $p = 0.007$), AMYm ($r_s = 0.57$, N = 22, $p = 0.006$), and TS ($r_s = 0.47$, N = 22, $p = 0.028$). Trends were also present for the NAcc ($r_s = 0.40$, N = 22, $p = 0.066$) and the POA ($r_s = 0.39$, N = 22, $p = 0.071$). There were no significant correlations or trends for any other target nuclei in relation to courtship ($p > 0.09$ for all). For aggression, solely one negative trend between aggression frequency (of any intensity) and Fos-ir density was present in the NAcc ($r = -0.38$, N = 22, $p = 0.074$, data not shown), with no other patterns present ($p > 0.11$ for all). All results of the correlation analyses are shown in Supplementary Table 1.

3.3. Co-variance in SDMN neural activity patterns across treatments

We next hypothesized that the three different experimental treatments would result in distinct neural activity patterns, as determined by covariance analysis of Fos-ir densities across SDMN nodes. When examining the functional connectivity across the entire SDMN, we found the mean ($\bar{x}$) correlation to be much stronger within subjects in the Reproductive opportunity ($\bar{x}r_s = 0.53$) than within Control treatment subjects ($\bar{x}r_s = 0.40$). Aggression treatment, contrastingly, caused a slight decrease in SDMN connectivity ($\bar{x}r_s = 0.33$) relative to the Control treatment.

We used hierarchical clustering on the correlation matrices of Fos-ir densities and behavioral measures, and discovered characteristic activity patterns for Reproductive, Agonistic, and Control treatments, with numerous clusters strongly supported by bootstrap resampling (Fig. 4). Importantly, across treatments, a shared core network emerged, most robustly in the Agonistic treatment, but still clearly visible in the other treatments as well. The network was not as robust within the Reproductive context, but it was most highly intercorrelated within this context. While the statistical support for some of the nodes as part of this network varied across treatment, this core network was characterized by synergistic Fos-ir densities in several nuclei of the amygdala-bed nucleus of the stria terminalis-lateral septum region as well as several hypothalamic regions. Interestingly, the activity of this network did not correlate with any behavioral measures (although select individual nodes did correlate with behavior as indicated above). Of note, the NAc was robustly recruited into this network only in the Agonistic context, whereas the AMYbl was no longer participating (Fig. 4A). Conversely, the PVN was robustly recruited only in the Reproductive context (Fig. 4B). Finally, activity of OT neurons in the SON and PVN became integrated into this core network only under social (Reproductive and Agonistic) conditions.

3.4. Functional connectivity of signaling molecule source node activity (Fos colocalization) with SDMN node activity (Fos density) and social behavior

The activity of neuron populations expressing signaling molecules – the catecholamines, nonapeptides, and 5-HT – showed remarkable differences across treatment groups. Differences in the activation of catecholaminergic circuits are particularly striking. For example, TH-ir cells in the VTA, RAs, RAi, and PH-AH formed a co-activation cluster in the Agonistic treatment only, in tight correlation with aggression intensity (Fig. 4A). In contrast, the involvement of catecholaminergic signaling appeared to be much less dependent on the raphe nuclei in the Reproductive treatment, where activation of TH-ir neurons in areas A8, SN, VTA, AH, and PH-AH was strongly correlated with the frequency and intensity of courtship displays (Fig. 4B). We observed much less co-activation of catecholamine populations in the Control treatment (Fig. 4C).

When we examined the involvement of nonapeptide neuron populations, we observed that the activity of OT neurons in the SON and PVN was integrated into the core network, as described above, only under social (Reproductive and Agonistic) conditions (Fig. 4). In striking contrast, the activity of the four VP neuron populations (in the BNST, PVN, SON, and POA) appeared to be largely uncorrelated with the activity of the core network or other source nodes (Fig. 4). 5-HT activity appeared to co-vary negatively with the activity of the core network in the Agonistic condition, but did not show any such correlation, nor with any behavioral measures, in the Reproductive and Control treatment conditions (Fig. 4).

Finally, we used hierarchical clustering on the correlation matrices that combine source node and target node activities across all treatments for each signaling molecule (Fig. 5). It is clear that the VP, 5-HT, and TH populations cluster primarily with each other and separately from the SDMN nodes. The one strong exception to this segregation is the inclusion of the OT populations (both PVN and SON) within the SDMN nodes. Furthermore, the catecholamines, VP, and 5-HT populations generally correlate negatively with SDMN activity.

4. Discussion

In the present study, we examined neural activation patterns across the SDMN and associated regions in the male brown anole, *Anolis sagrei*, within both Reproductive and Agonistic contexts. We then related this neural activity measure to the activity (as determined by colocalization with Fos) of different 'source' nodes that release neurotransmitters and neuropeptides that can modulate SDMN 'target' node activity. Overall, our results show that: (1) neural activity of a core network of SDMN nodes varies across social conditions; however, although activity at some nodes does correlate with behavioral output, in general the SDMN network activity seems largely unrelated to specific behavioral outputs; (2) functional connectivity of nodes within the SDMN varies across social contexts (the greatest mean connectivity is present during the Reproductive context, although a more robustly (though more weakly) connected cluster of nodes is present in the Agonistic challenge treatment); (3) the frequency and intensity of courtship and the intensity of aggressive behaviors correlate with activation of various catecholaminergic cell clusters in the hypothalamus, midbrain, and hindbrain; and (4) functional connectivity of source nodes to SDMN target nodes varies across type of signaling molecule and social condition – in general, activation of VP, catecholamines, and 5-HT are uncorrelated or negatively correlated to SDMN activity while OT activation is positively correlated to SDMN activity.

4.1. Between-treatment and within-treatment analyses of SDMN activity

When comparing SDMN activity across treatment groups, we surprisingly found that Fos-ir density is lower at several nodes following social encounter trials than in Control group subjects. These results were especially true for the Reproductive opportunity treatment and the LS, VMS, BNST-AMYm, and AMYbl—although the latter two nodes also showed significantly lower activity levels in the Agonistic group than Control group subjects. In contrast to these between-treatment findings of lower SDMN activity during social encounters, within-group analyses of Reproductive opportunity subjects instead revealed positive correlations between the number of courtship behaviors performed and Fos-ir densities, albeit in partly different nodes than those exhibiting between-treatment effects (BNST, BNST-AMYm, AMYm, and TS). Two potential explanations of these contrasting results seem possible.

First, encountering a novel conspecific in the proximity of one's territory may cause a general inhibition of SDMN activity during an initial investigative stage in order to prevent inappropriate behavioral output (e.g., to prevent courtship displays during an Agonistic challenge or aggressive displays during a Reproductive opportunity); the disinhibition of SDMN nodes may then allow for behavioral expression and thus account for the positive correlations between behavioral frequencies and SDMN activity. In partial support of this notion, Kollack-Walker and Newman (1995) found identical Fos-ir patterns in both

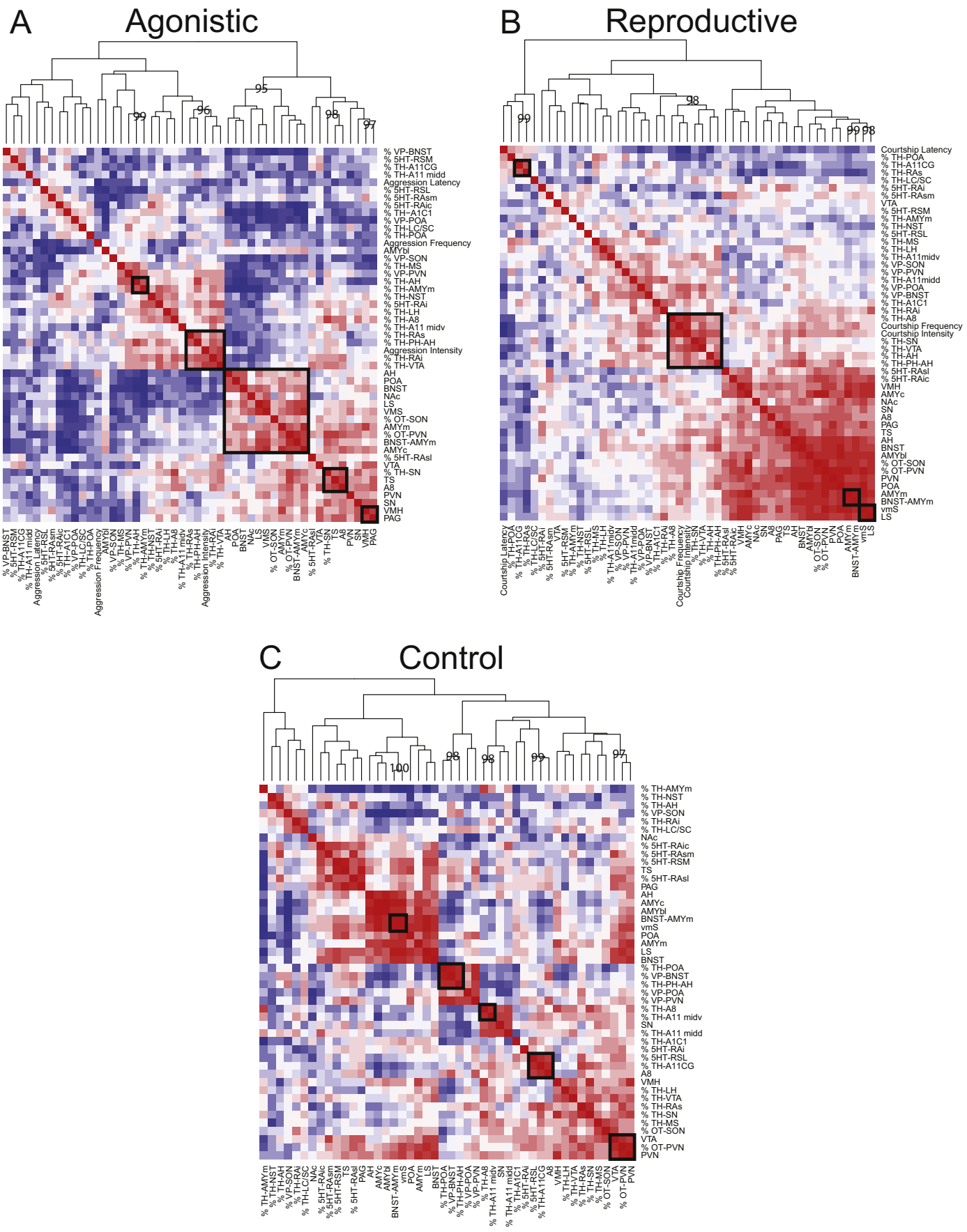

(caption on next page)

Fig. 4. Hierarchically clustered covariance matrices correlating behavioral measures with Fos-ir density across the SDMN, separated by Agonistic (A), Reproductive (B), and Control (C) treatments. Hierarchical clustering followed by permutation analysis reveals significant clusters (indicated by black boxes; $p < 0.05$). Forebrain and midbrain clusters of nodes are found to be significantly related across all treatment groups, although the included nodes vary somewhat across treatments. Importantly, the mean correlation across all SDMN nodes is greatest ($\bar{x}r_s = 0.53$) within the Reproductive context relative to the Control treatment group ($\bar{x}r_s = 0.40$), and lowest in the Agonistic treatment group ($\bar{x}r_s = 0.33$).

dominant male hamsters that attacked conspecifics and subordinate animals that performed defensive behaviors; the authors proposed that the agonistic context itself activates a "hardwired" circuitry associated with the context, and which may influence the probability of a behavior to be exhibited, but is independent of the actual performance of that behavior. These authors suggested that this general Fos-ir induction may simply be related to turning-on fight-or-flight circuitry, or general arousal. A similar general increase in Fos induction was also found in both winning and losing zebrafish, *Danio rerio*, within agonistic challenges (Teles et al., 2015). In our study, it is possible that the observed decrease in Fos-ir density at some SDMN nodes is due to a similar alteration to a general process, such as an initial inhibition of behavioral circuitry during social situation assessment as described above; alternately, the decrease in Fos expression observed in our study may be simply due to a suppression of inhibitory interneurons at these nodes, thus also leading to increased arousal or stimulation of stress circuitry. Further characterization of the activated SDMN neurons is necessary to distinguish among such possible explanations.

A second explanation for the contrasting directionality of results in the between-treatment and within-treatment analyses is simply that different nodes (other than the BNST-AMYm transition zone) were found to be significant in the first versus the second of these analyses, suggesting that different nodes have different types and valences of connectivity associated with social behavior profiles. Thus, whereas some nodes saw context-dependent decreases in Fos, others saw behavior-related increases in Fos expression. This is already somewhat predicted in models of the social behavior network whereby specific nodes see increases in activity, while other nodes see decreases or a lack of change in activity, within given social situations (Crews, 2003; Goodson, 2005; Newman, 1999). Furthermore, some nodes may respond in an all-or-none manner to a given social situation, while other nodes may be more integrated with behavioral frequency or intensity regulation, leading to further variability in functional connectivity among regions.

4.2. Functional connectivity within the SDMN: target node Fos density intercorrelations

Our $\bar{x}$ correlation comparison demonstrated that, globally, functional connectivity within the SDMN increased during Reproductive opportunities, relative to connectivity in Control group subjects. Furthermore, this analysis indicated a decrease in $\bar{x}$ correlation among SDMN nodes in Agonistic challenge subjects, relative to Control group subjects. These results are in accordance with Johnson et al. (2016) who found an increase in functional connectivity within a pair-bonding network in male prairie voles (*Microtus ochrogaster*) following mating relative to unmated control subjects. Our analyses similarly indicate that Reproductive opportunities increase the functional connectivity within social behavior regulating nodes, within an even greater array of SDMN nodes than those investigated in the vole study. Furthermore, our study examined subjects in an Agonistic challenge treatment, as well as a Reproductive opportunity treatment. The inclusion of an aggressive challenge treatment in our study was highly informative as it demonstrated that the observed increase in SDMN functional connectivity is specific for Reproductive opportunities and not social encounters of any type; in fact, our results suggest that Agonistic challenges slightly decrease connectivity of SDMN nodes, perhaps due to the recruitment of only a subset of these nodes, whereby Reproductive opportunities may recruit more of the network as a whole.

4.3. Functional connectivity of signaling molecule source nodes with SDMN target nodes

Our analyses of connectivity between activity in signaling molecule-producing neuron populations (source nodes) and activity in SDMN (target) nodes suggests contrasting associations of the SDMN with OT than with all other examined signaling molecules. We found that while VP, catecholamine, and 5HT activity were generally inversely related to SDMN activity, OT activity was positively related to network activity and clustered significantly with SDMN nodes.

The connectivity between source and target nodes also differed across treatment groups. OT activity clustered significantly with several BSNT nodes in the Agonistic context, and although non-significantly, even more strongly within the Reproduction context. In contrast, Control context animals showed OT connectivity solely with the VTA and PVN of the SDMN. No other source node phenotype showed strong positive connectivity with the SDMN. Instead, in the Agonistic context, there were strongly negative associations between catecholamines, VP, and 5HT with the SDMN. These associations were weakly negative to neutral within the Reproduction context, and highly variable within the Control context. These differences in connectivity may be due to alterations in neural activity at either the source nodes, target nodes, or both. The changes in target node activation are described above. The changes in source node activity have already been described in previous publications from our lab that examined brain tissues from these same subjects. As a summary, we have demonstrated increased VP-Fos and TH-Fos colocalization at a number of source nodes in the context of Reproductive and Agonistic challenges, as well as in a correlated manner with displayed courtship and aggressive behavior measures (Kabelik et al., 2013, 2014). OT-Fos colocalization also correlated positively with displayed courtship but not aggressive behaviors, but no effects of social treatment assignment were seen on OT-Fos colocalization (Kabelik and Magruder, 2014). In contrast to the activity increases described above, we generally observed decreased 5HT-Fos colocalization following both Reproductive and Agonistic treatments, relative to Control subjects, as well as negative correlations between 5-HT-Fos colocalization and measures of behavioral frequency and intensity (Hartline et al., 2017). Therefore, VP, OT, catecholamine, and 5HT release may all serve to regulate neural activity and connectivity within the SDMN.

The regulation of SDMN nodal activity and connectivity by hormonal and neurochemical signaling molecules is to be expected and we can therefore infer that at least some of the target node activity is attributable to our source node activity measures, despite these being correlational relationships (Crews, 2003; Goodson, 2005; Goodson and Kabelik, 2009; Newman, 1999; O'Connell and Hofmann, 2012; Yang and Wilczynski, 2002). For instance, previous research has directly demonstrated that OT can alter functional connectivity within a pair-bonding neural network that partly overlaps with the SDMN (Johnson et al., 2016). Future examination of these systems through pharmacological manipulations will allow us to establish causality of the various source node molecules on SDMN activity.

Neuropeptides such as OT and VP can have especially widespread effects on neural networks since they are often released via dendritic, axonal, and somatic release from large magnocellular neurons that were once thought to solely innervate the pituitary (Morris and Pow, 1991). This may be illustrated by the clustering of OT with the SDMN in the present study, suggesting widespread OT release and modulation of SDMN activity. On contrast, VP shows strong negative correlations to

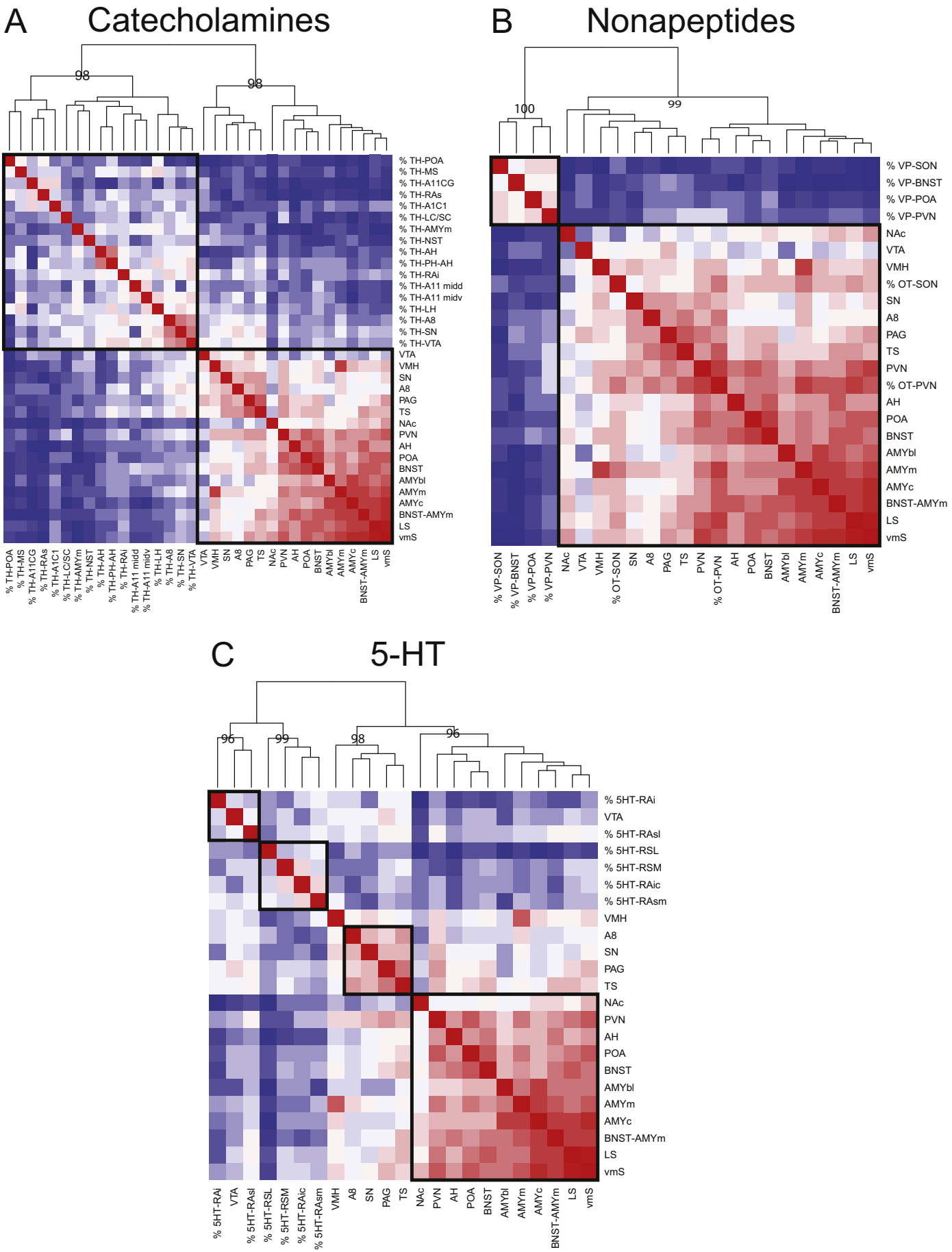

(caption on next page)

Fig. 5. Hierarchically clustered covariance matrices correlating source node populations with Fos-ir density across the SDMN (all three treatment groups combined), with data for (A) catecholamines, (B) nonapeptides, and (C) 5-HT shown separately. Hierarchical clustering followed by permutation analysis reveals significant clusters (indicated by black boxes; $p < 0.05$).

the SDMN activity and may thus suggest that VP may suppress SDMN activity. Despite great dilution due to extra-synaptic release, neuropeptides possess a long half-life and their receptors bind these ligands with high affinity, thus maintaining effectiveness of such signaling systems (Ludwig and Leng, 2006). Unlike traditional neurotransmitters that are released at synapses, neuropeptides diffusing through the central nervous system often act as neuromodulators that can exert subtle effects, such as the priming of secretory vesicles at release sites rather than their immediate release (Ludwig and Leng, 2006). Such priming (or similar mechanisms) may further explain differences in functional connectivity across social conditions. For instance, in some cases, release of the same signaling molecule is elevated in different social conditions, e.g., VP activation was increased at multiple source nodes in these same subjects within both Reproductive and Agonistic challenges (Kabelik et al., 2013); however, encountering an opposite-sex versus same-sex conspecific will likely cause differential activity in neurons that may all be similarly primed by vasopressin, thereby generating different connectivity patterns.

4.4. Connectivity of the social behavior and mesolimbic reward networks

Within our study, the majority of regions showing Fos induction differences between social environments and across levels of behavioral expression were nodes of the social behavior network (LS, BNST, BNST-AMYm transition region, AMYm), and those integrated primarily with this network due to their connections (VMS, TS). The lone exception to this pattern was the AMYbl, a component of the mesolimbic reward network with strong connections to the NAcc and VTA, and with known social behavior functions in reptiles (O'Connell and Hofmann, 2011b). Despite this relative lack of Fos induction within mesolimbic reward nodes in association with social context and behavioral expression, more cryptic changes within this network were detected when examining functional connectivity. The main finding in this regard is the presence of much stronger connectivity of the entire SDMN (including social behavior network nuclei and mesolimbic regions) during social behavior trials than during nonsocial Control conditions. Such an increase in forebrain connectivity to multiple mesolimbic regions strongly supports the notion of a functional SDMN in brown anole lizards.

4.5. The reptilian SDMN

Goodson and Kingsbury (2013) noted that the SDMN homologies proposed by O'Connell and Hofmann (2011b) were insufficiently supported for non-mammalian and non-avian vertebrates: "A second challenge in the extension of the SDM[N] model to non-mammalian taxa is that social behavior functions are unknown for the vast majority of SDM[N] components in non-mammalian taxa." Although some of the homologies that we present in the introduction are indeed putative, others are supported by many lines of functional, hodological, and chemoarchitectural evidence. We argue that the present results, especially when combined with limbic system involvement findings documented in Kabelik et al. (2014), provide support for a similar SDMN within reptiles as is present in other amniotes. Further evidence for an intact SDMN within non-mammalian and non-avian vertebrates comes from Teles et al. (2015), who demonstrate correlated immediate early gene induction across SDMN nodes within zebrafish, and these correlations were also found to vary with social context. Therefore, we argue that a functional SDMN is present within all vertebrate groups.

Acknowledgements

We would like to thank Rhodes College, as well as Dr. Charles and Mrs. Patricia Robertson, for their generous support of DK, SCC, JTH, and ANS. This work was supported by an NSF Graduate Research Fellowship to CAW and NSF grants IOS-1501704 to HAH and IOS-1601734 to CAW and HAH.

Appendix A. Supplementary data

Supplementary data to this article can be found online at https://doi.org/10.1016/j.yhbeh.2018.06.013.

References

Albers, H.E., 2015. Species, sex and individual differences in the vasotocin/vasopressin system: relationship to neurochemical signaling in the social behavior neural network. Front. Neuroendocrinol. 36, 49–71. https://doi.org/10.1016/j.yfrne.2014.07.001.

Altstein, M., Whitnall, M.H., House, S., Key, S., Gainer, H., 1988. An immunochemical analysis of oxytocin and vasopressin prohormone processing in vivo. Peptides 9, 87–105. https://doi.org/10.1016/0196-9781(88)90014-9.

Butler, A.B., Hodos, W., 2005. Comparative Vertebrate Neuroanatomy: Evolution and Adaptation. John Wiley & Sons.

Crawford, N.G., Parham, J.F., Sellas, A.B., Faircloth, B.C., Glenn, T.C., Papenfuss, T.J., Henderson, J.B., Hansen, M.H., Simison, W.B., 2015. A phylogenomic analysis of turtles. Mol. Phylogenet. Evol. 83, 250–257. https://doi.org/10.1016/j.ympev.2014.10.021.

Crews, D., 2003. The development of phenotypic plasticity: where biology and psychology meet. Dev. Psychobiol. 43, 1–10. https://doi.org/10.1002/dev.10115.

Distel, H., 1978. Behavior and electrical brain stimulation in the green iguana, *Iguana iguana* L. II. Stimulation effects. Exp. Brain Res. 31, 353–367. https://doi.org/10.1007/BF00237295.

Font, C., Martínez-Marcos, A., Lanuza, E., Hoogland, P.V., Martínez-García, F., 1997. Septal complex of the telencephalon of the lizard *Podarcis hispanica*. II. Afferent connections. J. Comp. Neurol. 383, 489–511. https://doi.org/10.1002/(SICI)1096-9861(19970714)383:4<489::AID-CNE7>3.0.CO;2-Z.

Font, C., Lanuza, E., Martinez-Marcos, A., Hoogland, P.V., Martinez-Garcia, F., 1998. Septal complex of the telencephalon of lizards: III. Efferent connections and general discussion. J. Comp. Neurol. 401, 525–548. https://doi.org/10.1002/(SICI)1096-9861(19981130)401:4<525::AID-CNE6>3.0.CO;2-Y.

Goodson, J.L., 2005. The vertebrate social behavior network: evolutionary themes and variations. Horm. Behav. 48, 11–22. https://doi.org/10.1016/j.yhbeh.2005.02.003.

Goodson, J.L., Kabelik, D., 2009. Dynamic limbic networks and social diversity in vertebrates: from neural context to neuromodulatory patterning. Front. Neuroendocrinol. 30, 429–441. https://doi.org/10.1016/j.yfrne.2009.05.007.

Goodson, J.L., Kingsbury, M.A., 2013. What's in a name? Considerations of homologies and nomenclature for vertebrate social behavior networks. Horm. Behav. 64, 103–112. https://doi.org/10.1016/j.yhbeh.2013.05.006.

Harrell, F.E., 2018. Hmisc: Harrell Miscellaneous. [WWW Document]. URL. http://cran.rproject.org/web/packages/Hmisc/index.html (accessed 4.13.18).

Hartline, J.T., Smith, A.N., Kabelik, D., 2017. Serotonergic activation during courtship and aggression in the brown anole, *Anolis sagrei*. PeerJ 5, e3331. https://doi.org/10.7717/peerj.3331.

Herdegen, T., Leah, J.D., 1998. Inducible and constitutive transcription factors in the mammalian nervous system: control of gene expression by Jun, Fos and Krox, and CREB/ATF proteins. Brain Res. Rev. 28, 370–490. https://doi.org/10.1016/S0165-0173(98)00018-6.

Hoffman, G.E., Smith, M.S., Verbalis, J.G., 1993. c-Fos and related immediate early gene products as markers of activity in neuroendocrine systems. Front. Neuroendocrinol. 14, 173–213. https://doi.org/10.1006/frne.1993.1006.

Johnson, Z.V., Walum, H., Jamal, Y.A., Xiao, Y., Keebaugh, A.C., Inoue, K., Young, L.J., 2016. Central oxytocin receptors mediate mating-induced partner preferences and enhance correlated activation across forebrain nuclei in male prairie voles. Horm. Behav. 79, 8–17. https://doi.org/10.1016/j.yhbeh.2015.11.011.

Kabelik, D., Magruder, D.S., 2014. Involvement of different mesotocin (oxytocin homologue) populations in sexual and aggressive behaviours of the brown anole. Biol. Lett. 10https://doi.org/10.1098/rsbl.2014.0566. (20140566).

Kabelik, D., Alix, V.C., Burford, E.R., Singh, L.J., 2013. Aggression- and sex-induced neural activity across vasotocin populations in the brown anole. Horm. Behav. 63, 437–446. https://doi.org/10.1016/j.yhbeh.2012.11.016.

Kabelik, D., Alix, V.C., Singh, L.J., Johnson, A.L., Choudhury, S.C., Elbaum, C.C., Scott, M.R., 2014. Neural activity in catecholaminergic populations following sexual and aggressive interactions in the brown anole, *Anolis sagrei*. Brain Res. 1553, 41–58. https://doi.org/10.1016/j.brainres.2014.01.026.

Kelly, A.M., Goodson, J.L., 2014. Social functions of individual vasopressin-oxytocin cell groups in vertebrates: What do we really know? Front. Neuroendocrinol. 35, 512–529. https://doi.org/10.1016/j.yfrne.2014.04.005.
Kabelik D., Hofmann H.A. Comparative neuroendocrinology: A call for more study of reptiles! Hormones and Behavior. This issue.
Kollack-Walker, S., Newman, S.W., 1995. Mating and agonistic behavior produce different patterns of Fos immunolabeling in the male Syrian hamster brain. Neuroscience 66, 721–736. https://doi.org/10.1016/0306-4522(94)00563-K.
Lanuza, E., Belekhova, M., Martínez-Marcos, A., Font, C., Martínez-García, F., 1998. Identification of the reptilian basolateral amygdala: an anatomical investigation of the afferents to the posterior dorsal ventricular ridge of the lizard *Podarcis hispanica*. Eur. J. Neurosci. 10, 3517–3534. https://doi.org/10.1046/j.1460-9568.1998.00363.x.
Lee, A.G., Cool, D.R., Grunwald, W.C., Neal, D.E., Buckmaster, C.L., Cheng, M.Y., Hyde, S.A., Lyons, D.M., Parker, K.J., 2011. A novel form of oxytocin in New World monkeys. Biol. Lett. 7, 584–587. https://doi.org/10.1098/rsbl.2011.0107.
Ludwig, M., Leng, G., 2006. Dendritic peptide release and peptide-dependent behaviours. Nat. Rev. Neurosci. 7, 126–136.
Martínez-García, F., Martínez-Marcos, A., Lanuza, E., 2002. The pallial amygdala of amniote vertebrates: evolution of the concept, evolution of the structure. Brain Res. Bull. 57, 463–469. https://doi.org/10.1016/S0361-9230(01)00665-7.
Morrell, J.I., Crews, D., Ballin, A., Morgentaler, A., Pfaff, D.W., 1979. 3H-estradiol, 3H-testosterone and 3H-dihydrotestosterone localization in the brain of the lizard *Anolis carolinensis*: an autoradiographic study. J. Comp. Neurol. 188, 201–223. https://doi.org/10.1002/cne.901880202.
Morris, J.F., Pow, D.V., 1991. Widespread release of peptides in the central nervous system: quantitation of tannic acid-captured exocytoses. Anat. Rec. 231, 437–445. https://doi.org/10.1002/ar.1092310406.
Newman, S., 1999. The medial extended amygdala in male reproductive behavior. Ann. N. Y. Acad. Sci. 242–257.
O'Connell, L.A., Hofmann, H.A., 2011a. Genes, hormones, and circuits: an integrative approach to study the evolution of social behavior. Front. Neuroendocrinol. 32, 320–335. https://doi.org/10.1016/J.YFRNE.2010.12.004.
O'Connell, L.A., Hofmann, H.A., 2011b. The vertebrate mesolimbic reward system and social behavior network: a comparative synthesis. J. Comp. Neurol. 519, 3599–3639. https://doi.org/10.1002/cne.22735.
O'Connell, L.A., Hofmann, H.A., 2012. Evolution of a vertebrate social decision-making network. Science 336, 1154–1157. https://doi.org/10.1126/science.1218889. (80-.).
Rittschof, C.C., Robinson, G.E., 2016. Behavioral genetic toolkits: toward the evolutionary origins of complex phenotypes. Curr. Top. Dev. Biol. 119, 157–204. https://doi.org/10.1016/BS.CTDB.2016.04.001.
Sabatier, N., Caquineau, C., Dayanithi, G., Bull, P., Douglas, A.J., Guan, X.M.M., Jiang, M., Van der Ploeg, L., Leng, G., 2003. α-Melanocyte-stimulating hormone stimulates oxytocin release from the dendrites of hypothalamic neurons while inhibiting oxytocin release from their terminals in the neurohypophysis. J. Neurosci. 23, 10351 (LP-10358).
Schindelin, J., Arganda-Carreras, I., Frise, E., Kaynig, V., Longair, M., Pietzsch, T., Preibisch, S., Rueden, C., Saalfeld, S., Schmid, B., Tinevez, J.-Y., White, D.J., Hartenstein, V., Eliceiri, K., Tomancak, P., Cardona, A., 2012. Fiji: an open-source platform for biological-image analysis. Nat. Methods 9, 676–682.
Suzuki, R., Shimodaira, H., 2006. Pvclust: an R package for assessing the uncertainty in hierarchical clustering. Bioinformatics 22, 1540–1542.
Taborsky, M., Hofmann, H.A., Beery, A.K., Blumstein, D.T., Hayes, L.D., Lacey, E.A., Martins, E.P., Phelps, S.M., Solomon, N.G., Rubenstein, D.R., 2015. Taxon matters: promoting integrative studies of social behavior: NESCent working group on integrative models of vertebrate sociality: evolution, mechanisms, and emergent properties. Trends Neurosci. 38, 189–191. https://doi.org/10.1016/J.TINS.2015.01.004.
Teles, M.C., Almeida, O., Lopes, J.S., Oliveira, R.F., 2015. Social interactions elicit rapid shifts in functional connectivity in the social decision-making network of zebrafish. Proc. R. Soc. B Biol. Sci. 282.
Yang, E.-J., Wilczynski, W., 2002. Relationships between hormones and aggressive behavior in green anole lizards: an analysis using structural equation modeling. Horm. Behav. 42, 192–205. https://doi.org/10.1006/hbeh.2002.1811.